Molecular Order and Dynamics in Bilayers Consisting of Highly Polyunsaturated Phospholipids

Drake C. Mitchell and Burton J. Litman

Section of Fluorescence Studies, Laboratory of Membrane Biophysics and Biochemistry, National Institute on Alcohol Abuse and Alcoholism, National Institutes of Health, Rockville, Maryland 20852 USA

ABSTRACT   The time-resolved fluorescence emission and decay of fluorescence anisotropy of 1,6-diphenyl-1,3,5-hexatriene (DPH) was used to characterize equilibrium and dynamic bilayer structural properties of symmetrically substituted phosphatidylcholines (PCs) with acyl chains containing no, one, four, or six double bonds and mixed-chain phosphatidylcholines with a saturated sn-1 chain and one, four, or six double bonds in the sn-2 chain. Both the Brownian rotational diffusion (BRD) model and the wobble-in-cone model were fit to all differential polarization data, and the descriptions of the data provided by the BRD model were found to be statistically superior. Global analysis of differential polarization data revealed two statistically equivalent solutions. The solution corresponding to a bimodal orientational distribution function, $f(\theta)$, was selected based on the effects of temperature on $f(\theta)$ and previous measurements on fixed, oriented bilayers. The overall equilibrium acyl chain order in these bilayers was analyzed by comparing the orientational probability distribution for DPH, $f(\theta)$ sin θ, with a random orientational distribution. Orientational order decreased and probe dynamics increased in mixed-chain species as the unsaturation of the sn-2 chain was increased. The degree of orientational order dropped dramatically in the dipolyunsaturated species compared with the mixed-chain phosphatidylcholines, which contained a polyunsaturated sn-2 chain. In terms of both orientational order and probe dynamics, the differences between the highly polyunsaturated species and the monounsaturated species were much greater than the differences between the monounsaturated species and a disaturated PC.

INTRODUCTION

Phosphatidylcholines with two saturated acyl chains are among the most heavily studied of all phospholipids; however, these species are a minor constituent of most biological membranes. The phospholipids of most biological membranes are predominantly sn-1-saturated, sn-2-unsaturated, and many membranes contain notable levels of phospholipid species in which both acyl chains are polyunsaturated. High levels of acyl chain unsaturation are especially prevalent in the membranes of the nervous system, retina, and spermatozoa (Salem, 1986). Extensive fatty acid analysis (Miljanich et al., 1979) and phospholipid molecular species characterization (Stinson et al., 1991) of the bovine retina reveal that more than half of the fatty acid chains are docosahexaenoic acyl chains (22:6n3), and one-fourth of the phospholipids are dipolyunsaturated, containing two 22:6n3 acyl chains. The abundance of highly polyunsaturated phospholipids in biological membranes that perform a variety of crucial functions makes it imperative that we understand the unique properties they confer upon phospholipid bilayers.

It is widely recognized that phospholipid acyl chain unsaturation plays a major role in determining many important bilayer properties, including phase transition temperature (Niebylski and Salem, 1994; Kariel et al., 1991), bilayer thickness (Thurmond et al., 1994), area per molecule (Holte et al., 1995), and acyl chain packing free volume (Straume and Litman, 1987a). Measurements with a wide variety of techniques have led to a consensus that the introduction of a single *cis* double bond to a saturated acyl chain results in a large decrease in molecular order in the liquid crystalline phase. However, the effects of higher levels of unsaturation are not as widely agreed upon, and appear to vary, depending on the specific location of the double bonds and on whether one or both phospholipid acyl chains are unsaturated. Knowledge of the effects of acyl chain unsaturation on bilayer properties is especially incomplete for high levels of polyunsaturation, meaning four or more double bonds. It is not clear that the effects of a single double bond on acyl chain packing lead to any general description that can be used to explain the effects of high levels of polyunsaturation. Phospholipids with high levels of acyl chain unsaturation (four or more double bonds) have received relatively little study compared to phospholipids that are disaturated or monounsaturated. One aspect of the role of phospholipid acyl chain unsaturation in determining bilayer properties that remains relatively unexplored is the effect on molecular

order of high levels of unsaturation at both the *sn*-1 and *sn*-2 positions.

We report here a systematic examination of the effects of increasing unsaturation from one to six carbon-carbon double bonds, in one or both phospholipid acyl chains, on acyl chain packing in L-C phase bilayers. The effects of increasing unsaturation at only the *sn*-2 position was examined for the series 16:0, 18:1 PC; 16:0, 20:4 PC; and 16:0, 22:6 PC. The gel-LC phase transition temperatures for these three molecules are −2.5°C, −20.6°C, and −11.3°C, respectively (Hernandez-Borrell and Keough, 1993). The structures of the three unsaturated fatty acid acyl chains are shown in Fig. 1. In addition, the effects of increasing unsaturation of both acyl chains was studied for the series di-14:0, di-18:1 PC, di-20:4 PC, and di-22:6 PC. The gel-LC phase transition temperatures for these four molecules are 23 to 24°C (Caffrey, 1993), −16 to −20°C (Caffrey, 1993), −69°C (Kariel et al., 1991), and −68°C (Kariel et al., 1991), respectively. Examination of the set of six unsaturated molecules has facilitated differentiation of bilayer properties resulting from high levels of unsaturation on a single acyl chain from those due to unsaturation of both phospholipid acyl chains.

The time-resolved anisotropy decay of the fluorescent membrane probe DPH has been used by a large number of investigators to characterize acyl chain packing properties and phase transitions in biological membranes and phospholipid bilayers (see Lentz, 1993, for a review). A number of models have been employed to extract information about probe dynamics and orientational order from the anisotropy decay. We are primarily interested in the packing of the acyl chains in the bilayer, which will be reflected by the orientational order of a free tumbling probe such as DPH. It has been established both theoretically (van der Meer et al., 1984; Szabo et al., 1984) and experimentally (Ameloot et al., 1984; van Langen et al., 1987b, 1989; Wang et al., 1991) that the second- and fourth-rank order parameters $\langle P_2 \rangle$ and $\langle P_4 \rangle$ can be obtained from the decay of fluorescence anisotropy of DPH in randomly oriented membrane systems. To maximize the information gained from such measurements, the derived order parameters are generally used to calculate an equilibrium orientational distribution function, $f(\theta)$, of the fluorescent probe molecule. To facilitate comparisons of different bilayer compositions in terms of $f(\theta)$, we have calculated the overlap between the resulting probability distributions, $f(\theta) \sin \theta$, and a random distribution, and
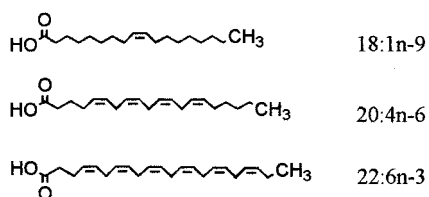
compare the resulting values with f_v, which has previously been used by this laboratory to summarize the DPH equilibrium orientational order (Straume and Litman, 1987a).

EXPERIMENTAL PROCEDURES

Sample preparation

All phospholipids were purchased from Avanti Polar Lipids (Alabaster, AL) and, after purity was checked by high-performance liquid chromatography, were used without further purification. DPH was purchased from Molecular Probes (Eugene, OR), dissolved in THF, and stored under argon at −20°C. Large unilamellar vesicles were prepared as follows. Lipid stock solutions were dried from chloroform under a stream of argon gas, and the resulting phospholipid film was dissolved in cyclohexane. The cyclohexane solution was frozen, then lyophilized to yield phospholipid in the form of a dispersed white powder. This powder was dissolved in a solution of octylglucoside (30 mM octylglucoside, 10 mM PIPES, 50 μM DTPA, pH 7.0). Octylglucoside was removed by dialysis against a 50-fold excess buffer a total of three times. The size distribution of the resulting large unilamellar vesicles was reduced by extrusion 10 times through a pair of 0.2-μm membranes with a Lipex extruder (Vancouver, BC). All buffers were heavily flushed with argon, and all preparative procedures involving unsaturated phospholipids were carried out in an argon-filled glove box. Samples for fluorescence measurements were made immediately before use by diluting a concentrated vesicle stock solution to 100 μM phospholipid, and adding 0.5 μl of DPH in THF to yield a final phospholipid/DPH ratio of 500:1. Argon was streamed into the cuvette during this entire process, and the added THF was allowed to evaporate by continuing the argon stream for several minutes after the addition of DPH. All samples were incubated at 40°C in darkness for 1 h before being brought to the required temperature for measurement. Total optical density (vesicle scatter plus absorption) at the wavelength of fluorescence excitation was less than 0.1.

Fluorescence measurements

Fluorescence lifetime and differential polarization measurements were performed with a K2 multifrequency cross-correlation phase fluorometer (ISS, Urbana, IL). Excitation at 351 nm was provided by an Innova 307 argon ion laser (Coherent, Santa Clara, CA). Lifetime and differential polarization data were acquired using decay acquisition software from ISS at 10, 20, 30, and 40°C, except for di-14:0 PC, which was studied at 30, 40, 47, and 55°C. For lifetime measurements 12 modulation frequencies were used, logarithmically spaced from 5 to 250 MHz. All lifetime measurements were made with the emission polarizer at the magic angle of 54.7° relative to the vertically polarized excitation beam and with POPOP in absolute ethanol in the reference cuvette (τ = 1.35 ns; Lakowicz et al., 1981). Differential polarization measurements were made at 15 modulation frequencies logarithmically spaced from 5 to 300 MHz. For each differential polarization measurement the instrumental polarization factors were measured and found to be between 1 and 1.05, and the appropriate correction factor was applied. Scattered excitation light was removed from the emission beam by a 390-nm highpass filter in the emission beam. At each frequency data were accumulated until the standard deviations of the phase and modulation ratio were below 0.2° and 0.004, respectively, and these values were used as the standard deviation for the measured phase and modulation ratio in all analysis. Both total intensity decay and differential polarization measurements were repeated at each temperature with each phospholipid a minimum of three times.

FIGURE 1 Structures of the three unsaturated fatty acid acyl chains investigated.

Data analysis

Total fluorescence intensity decays were modeled with a Lorentzian distribution, plus a discrete exponential decay to account for scattered back-

ground light, using Globals Unlimited (Alcala et al., 1987; Beechem et al., 1991). The lifetime of the discrete component was fixed at 0.001 ns, and its fractional intensity was allowed to vary along with the center of the Lorentzian distribution, τ_c, the width of the distribution at half height, w, and its fractional intensity. The resulting fractional intensity of the discrete component varied from 1% to less than 0.1%, and the values of reduced χ^2 ranged from 1 to 5.

Measured polarization-dependent differential phases and modulation ratios for each sample were combined with the measured total intensity decay to yield the anisotropy decay, $r(t)$. Anisotropy decays were analyzed using three different models: a sum of two discrete exponential decays, the wobble-in-cone model (Lipari and Szabo, 1981; Kinosita et al., 1977), and the BRD (Brownian rotational diffusion) model (see Levine and van Ginkel, 1994, for a review). Each of these models was used in a global analysis of all of the data at all four temperatures for a given phospholipid composition with r_0, the anisotropy at time 0, globally linked.

An empirical description of all anisotropy decays was obtained via analysis in terms of a simple sum of exponentials, of the form

$$r(t) = (r_o - r_\infty)(\beta_1 \exp(-t/\phi_1) + \beta_2 \exp(-t/\phi_2)) + r_\infty \quad (1)$$

Where r_o is the fluorescence anisotropy at $t = 0$, and r_∞ is the nondecaying anisotropy. F tests of the analysis of single experiment results showed that the data supported the use of five independent parameters (ϕ_1, ϕ_2, β_1, β_2, and r_∞) for the sum-of-exponentials model.

The empirical sum-of-exponentials model provides information about fluorophore rotational correlation times and the extent to which the fluorescence anisotropy can decay to zero. However, it provides no information regarding the range of equilibrium angular orientations DPH is restricted to by the surrounding matrix of phospholipid acyl chains. The equilibrium orientational distribution of a free-tumbling fluorescent probe molecule will reflect the equilibrium orientational order of the surrounding phospholipid acyl chains; therefore all data were also analyzed by using the BRD model, which yields the order parameters $\langle P_2 \rangle$ and $\langle P_4 \rangle$, which can be used to construct an orientational distribution function, $f(\theta)$, of the probe molecule.

The BRD model is based upon an approximate solution of the Smoluchowski equation (van der Meer et al. 1984; Szabo, 1984) and provides a theoretical framework for examining the orientational distribution of a free-tumbling fluorescent probe with cylindrical symmetry. In general the orientation of a molecule with cylindrical symmetry in a lipid bilayer is completely described by the angle θ between its symmetry axis and the local membrane normal. The generalized orientational distribution function, $f(\theta)$, can be written as a series expansion of the Legendre polynomials, $P_n(\cos \theta)$:

$$f(\theta) = \sum_n \frac{1}{2} (2n + 1)\langle P_n \rangle P_n(\cos \theta) \quad (2)$$

where n is even and $\langle P_n \rangle$ is the nth rank orientational order parameter. Order parameters are calculated according to

$$\langle P_n \rangle = \int_0^\pi (\sin \theta) f(\theta) P_n(\cos \theta) \mathrm{d}\theta \quad (3)$$

which follows from the fact that the Legendre polynomials are orthogonal.

For measurements on macroscopically isotropic systems, such as vesicle suspensions, only the first two order parameters, $\langle P_2 \rangle$ and $\langle P_4 \rangle$, can be extracted from the experimental data because of the symmetry of the dipole transition. The Brownian rotational diffusion (BRD) model relates the order parameters $\langle P_2 \rangle$ and $\langle P_4 \rangle$, the diffusion coefficient of the symmetry axis of the molecule, $D_\perp$, and r_0 to the observed anisotropy decay according to (van der Meer et al., 1984)

$$r(t) = r_0 \left(\sum_{i=1}^3 g_i \exp(-t/\phi_i) + g_4 \right) \quad (4)$$

where

$$g_1 = \frac{1}{5} + \frac{2}{7}\langle P_2 \rangle + \frac{18}{35}\langle P_4 \rangle - \langle P_2 \rangle^2$$

$$g_2 = \frac{2}{5} + \frac{2}{7}\langle P_2 \rangle - \frac{24}{35}\langle P_4 \rangle$$

$$g_3 = \frac{2}{5} - \frac{4}{7}\langle P_2 \rangle + \frac{6}{35}\langle P_4 \rangle$$

$$g_4 = \langle P_2 \rangle^2$$

$$\phi_1 = g_1 \Big/ \left[6D_\perp \left(\frac{1}{5} + \frac{\langle P_2 \rangle}{7} - \frac{12}{35}\langle P_4 \rangle \right) \right]$$

$$\phi_2 = g_2 \Big/ \left[12D_\perp \left(\frac{1}{5} + \frac{\langle P_2 \rangle}{14} + \frac{8}{35}\langle P_4 \rangle \right) \right]$$

$$\phi_3 = g_3 \Big/ \left[12D_\perp \left(\frac{1}{5} - \frac{\langle P_2 \rangle}{7} - \frac{2}{35}\langle P_4 \rangle \right) \right]$$

The recovered values of $\langle P_2 \rangle$ and $\langle P_4 \rangle$, along with the corresponding Legendre polynomials, can be used to construct the orientational distribution function according to Eq. 2. However, the resulting truncated series can produce negative values of $f(\theta)$. Therefore, interpretation of the recovered values of $\langle P_2 \rangle$ and $\langle P_4 \rangle$ in terms of an orientational distribution function requires adoption of a specific functional form for $f(\theta)$, which must satisfy the general constraints

$$f(\theta) \geq 0 \quad (5a)$$

$$\int_0^\pi f(\theta)\sin \theta \, \mathrm{d}\theta = 1 \quad (5b)$$

The order parameters $\langle P_2 \rangle$ and $\langle P_4 \rangle$ are related to $f(\theta)$ via two coupled integral equations of the type shown in Eq. 3, which means that $f(\theta)$ can include no more than two adjustable parameters.

The results of the BRD model-based analysis were interpreted in terms of an angular distribution function that is symmetrical about $\theta = \pi/2$, and is based on maximizing the information entropy of $f(\theta)$ (van der Meer et al., 1982; Pottel et al., 1986),

$$f(\theta) = N^{-1}\exp[\lambda_2 P_2(\cos \theta) + \lambda_4 P_4(\cos \theta)] \quad (6)$$

where λ_2 and λ_4 are constants determined by simultaneous solution of equations for $\langle P_2 \rangle$ and $\langle P_4 \rangle$ according to Eq. 3, and N is the normalization constant determined according to Eq. 5b.

A large number of factors, including changes in phospholipid acyl chain composition (Straume and Litman, 1987a,b; van Ginkel et al., 1989; Wang et al., 1991), have been shown to alter $f(\theta)$. One of the primary goals of this study is to assess the extent to which acyl chain unsaturation alters acyl chain packing. In this context it is useful to calculate a single parameter that corresponds to the extent to which the equilibrium orientational freedom of DPH is restricted by the phospholipid acyl chains. Straume and Litman

(1987a) have formulated such a parameter, f_v, which is defined by

$$f_v = \frac{1}{2 \times f(\theta)_{max}} \qquad (7)$$

when $f(\theta)$ is defined as a normalized distribution according to Eq. 5b. In the present study a new, more direct comparison of $f(\theta)$ and a random distribution was formulated. The parameter f_{random} is the overlap of the orientational probability distribution, $f(\theta) \sin \theta$, and a random orientational distribution, $f_{rand}(\theta) \sin \theta$:

$$f_{random} = 1 - \frac{1}{2} \int_0^\pi \left| f(\theta) - f(\theta)_{rand} \right| \sin \theta \, d\theta \qquad (8)$$

where $f_{rand}(\theta)$ is given by Eq. 6, with $\lambda_2 = \lambda_4 = 0$.

This parameter has the advantage that it results from a direct comparison with a random orientational distribution over the entire angular range from 0 to π, rather than depending upon the maximum value of $f(\theta)$ over that range. The ability of f_{random} and f_v to provide information regarding alterations in the orientational freedom of DPH due to changes in temperature and acyl chain composition were compared.

All analysis of differential polarization data was performed with NON-LIN (Dr. Michael Johnson, Pharmacology Department, University of Virginia Health Sciences Center, Charlottesville, VA), which uses a modified Gauss-Newton nonlinear least-squares algorithm (Straume et al., 1991; Johnson and Faunt, 1992), with subroutines specifying the fitting function written by the authors. NONLIN accounts for all higher order correlations that may exist between fitting parameters when confidence intervals are determined. The NONLIN software package allows the user to include a subroutine that calculates the most probable values and asymmetrical confidence intervals of quantities that are calculated from the designated fitting parameters. Use of this subroutine ensures the accurate propagation of confidence intervals when derived parameters are calculated from fitting parameters, for example, when calculating f_v and f_{random}. Asymmetrical confidence intervals equivalent to one standard deviation were obtained for both fitting variables and derived parameters. The values of χ^2 reported in Table 2 for the analysis of the differential polarization data are weighting factor corrected values. These were obtained by dividing the value of χ^2 obtained with each analytical model by the value of χ^2 obtained with the very best empirical solution. The best empirical solution was a sum-of-three-exponentials model, as this provided a significant improvement in χ^2 over a sum-of-two-exponentials model for some bilayer compositions.

RESULTS AND DISCUSSION

Fluorescence lifetimes

Total fluorescence decay data for all bilayer compositions and temperatures were analyzed with a Lorentzian distribution. The distribution centers, τ_c, given in Table 1, show the variation in DPH total intensity decay induced by changes in temperature and bilayer phospholipid composition. The effect of temperature varied with acyl chain composition. In di-22:6 PC, τ_c decreased by only 0.4 ns as the temperature changed from 10 to 40°C, whereas in 16:0, 18:1 PC, this temperature change lowered τ_c by more than 1.5 ns. Table 1 also shows that the value of τ_c depends strongly on bilayer composition and is generally smaller with increased unsaturation, with the three symmetrically unsaturated species having smaller values of τ_c than the species with one or more saturated chains. For each bilayer composition, τ_c decreases with temperature, which is consistent with the observed increase in water penetration into the bilayer with increasing temperature (Bernsdorff et al., 1997). The large isothermal variation in τ_c with bilayer composition is consistent with recent measurements which showed that water penetration into the bilayer increases in the order 18:0,18:1 PC $<$ 18:0,22:6 PC $<$ di-22:6 PC, and the water permeability coefficient for di-22:6 PC is ~6 times greater than that for 18:0,18:1 PC (Huster et al., 1997).

Another possible cause of the large variation in τ_c with temperature and composition is the dependence of membrane probe fluorescence lifetime on probe orientational order and the index of refraction of the bilayer (Toptygin et al., 1992; Toptygin and Brand, 1993). The dependence of fluorescence lifetime on orientational order could account for some of the temperature-dependent variation in τ_c. With an index of refraction of 1.425 for the bilayer (Toptygin and Brand, 1993), the relationships of Toptygin and Brand (1993) show that a decrease in $\langle P_2 \rangle$ from 0.4 to 0.25 would decrease the fluorescence lifetime by less than 0.2 ns; thus

TABLE 1   Centers, τ_c,* and widths, w,* of Lorentzian distributions of DPH fluorescence intensity decay

Phospholipid		10°C	20°C	30°C	40°C
di-22:6n3 PC	τ_c	6.79 ± 0.10	6.58 ± 0.13	6.50 ± 0.10	6.41 ± 0.12
	w	1.79 ± 0.16	1.69 ± 0.21	1.60 ± 0.21	1.84 ± 0.23
di-20:4n6 PC	τ_c	7.92 ± 0.12	7.63 ± 0.08	7.59 ± 0.19	7.13 ± 0.10
	w	2.22 ± 0.08	1.81 ± 0.16	1.34 ± 0.22	1.68 ± 0.20
di-18:1n9 PC	τ_c	8.0 ± 0.10	7.71 ± 0.08	7.34 ± 0.08	6.94 ± 0.08
	w	0.38 ± 0.05	0.17 ± 0.08	0.40 ± 0.20	0.71 ± 0.10
16:0,22:6n3 PC	τ_c	8.57 ± 0.06	8.32 ± 0.16	7.95 ± 0.09	7.41 ± 0.08
	w	0.27 ± 0.02	0.37 ± 0.10	0.49 ± 0.04	0.81 ± 0.09
16:0, 20:4n6 PC	τ_c	8.51 ± 0.21	8.23 ± 0.23	7.76 ± 0.08	7.7 ± 0.07
	w	0.81 ± 0.18	0.79 ± 0.29	1.03 ± 0.25	1.58 ± 0.21
16:0, 18:1n9 PC	τ_c	9.62 ± 0.18	9.20 ± 0.09	8.64 ± 0.12	8.10 ± 0.10
	w	0.40 ± 0.40	0.61 ± 0.25	0.78 ± 0.20	0.93 ± 0.24
di-14:0 PC	τ_c	—#	—#	8.85 ± 0.10	7.85 ± 0.08
	w			0.27 ± 0.04	0.21 ± 0.06

*Units of nanoseconds (ns).
#Not measured.

changes in orientational order could account for 10–20% of the temperature-induced variation in τ_c. It is conceivable that the variation in τ_c with lipid composition could be related to changes in index of refraction; for example, the index of refraction of arachidonic acid is 1.482 and that of myristic acid is 1.4305. The relationships of Toptygin and Brand (1993) show that with $\langle P_2 \rangle = 0.3$ this difference in index of refraction would lead to a τ for di-14:0 PC ~0.5 ns shorter than that for di-20:4 PC; however, the measured τ_c for di-14:0 PC is 0.7–1.3 ns longer than that for di-20:4 PC. These calculations underline the importance of water penetration in determining the fluorescence lifetime of hydrophobic bilayer probes and further suggest that the range of values of τ_c shown in Table 1 is most likely due to bilayer composition and temperature-induced changes in water penetration.

The widths of the lifetime distributions, w, also vary with temperature and composition. The values of w fall into two general categories, with w greater than 1.5 ns for di-22:6 PC and di-20:4 PC, whereas w is generally less than 1 ns for all other phospholipids. The width of the lifetime distribution is indicative of the relative homogeneity of the bilayer environment of the probe molecule (Bernsdorff et al., 1997). A positive correlation between w and environmental heterogeneity is reflected in the increase in w with increasing temperature observed for most of the phospholipids. Comparison of the values of w in Table 1, especially those for 10°C, show that DPH in the two dipolyunsaturated phospholipids experiences the highest level of environmental heterogeneity. The values of w in Table 1 indicate that DPH in the two dipolyunsaturated species at 10°C experiences a greater degree of environmental heterogeneity than DPH in any of the other species at 40°C.

Anisotropy decays

The DPH differential polarization data obtained at all four temperatures were simultaneously globally analyzed in terms of a sum of two exponential decays plus the residual anisotropy at infinite time (Eq. 1), with r_o globally linked. The values of χ^2 obtained by this global analysis demonstrate that Eq. 1 provides a good, empirical description of the decay of DPH fluorescence anisotropy in all of the bilayer compositions studied, as shown in Table 2. Although two rotational correlation times were required for an adequate description of all anisotropy decay data, there is no physical basis for assigning a particular meaning to the individual rotational correlation times. Therefore, changes in total rotational rates of DPH were compared in terms of the average rotational correlation time $\langle \phi \rangle$, defined as $\langle \phi \rangle = (\beta_1 \phi_1 + \beta_2 \phi_2)/(r_o - r_\infty)$. In all phospholipid compositions increasing temperature reduced $\langle \phi \rangle$, and this effect is most pronounced in the species with one or more saturated acyl chains (Fig. 2). The effect of this trend is that the ~4 ns variation in $\langle \phi \rangle$ found among all species at 10°C is reduced to ~1 ns at 40°C. One striking aspect of Fig. 2 is the essentially identical values of $\langle \phi \rangle$ for 16:0, 18:1 PC, di-18:1 PC, and di-14:0 PC over the temperature range from 10°C to 40°C. This similarity indicates that a double bond at the c9 position of the sn-2 chain or both chains has only a small effect on DPH rotational dynamics in the LC phase. Additional unsaturation of the sn-2 chain, or both chains, to the level of 20:4n6 and 22:6n3 progressively increases DPH rotational rates. The two dipolyunsaturated species had the lowest values of $\langle \phi \rangle$. The effect of acyl chain unsaturation on DPH rotational rates indicates that in the LC state high levels of unsaturation are necessary to cause an appreciable departure from the behavior observed in a disaturated phospholipid. In particular, unsaturation of both acyl chains with a single c9 cis double bond does not produce a bilayer environment that affords DPH as much rotational mobility as high levels of polyunsaturation at only the sn-2 acyl chain.

Although the sum-of-exponentials model provided a statistically valid description of the data, this model is rather unsatisfactory because it furnishes no information regarding the degree of orientational constraint imposed upon DPH by the surrounding matrix of phospholipid acyl chains. There-

TABLE 2 Global analysis of differential polarization data: values of r_o and χ^2

| Phospholipid		Sum of two exponentials + r_∞	Wobble-in-cone model	BRD model, high $\langle P_4 \rangle$ solution	BRD model, low $\langle P_4 \rangle$ solution
di-22:6n3	r_o	0.339 (0.005, 0.005)	0.317 (0.004, 0.004)	0.352 (0.009, 0.011)	0.354 (0.01, 0.012)
	χ^2	1.13	2.71	1.16	1.27
di-20:4n6	r_o	0.342 (0.002, 0.003)	0.332 (0.003, 0.003)	0.306 (0.003, 0.003)	0.307 (0.002, 0.002)
	χ^2	1.63	2.11	1.06	1.05
di-18:1n9	r_o	0.376 (0.003, 0.003)	0.338 (0.004, 0.005)	0.361 (0.003, 0.003)	0.362 (0.003, 0.003)
	χ^2	1.31	6.52	1.25	1.19
16:0, 22:6n3	r_o	0.334 (0.003, 0.003)	0.312 (0.005, 0.005)	0.339 (0.005, 0.006)	0.341 (0.006, 0.007)
	χ^2	1.13	10.2	1.21	1.79
16:0, 20:4n6	r_o	0.364 (0.004, 0.004)	0.340 (0.003, 0.004)	0.359 (0.003, 0.003)	0.359 (0.003, 0.003)
	χ^2	1.07	9.79	1.40	1.29
16:0, 18:1n9	r_o	0.357 (0.005, 0.005)	0.328 (0.004, 0.004)	0.355 (0.004, 0.005)	0.358 (0.004, 0.005)
	χ^2	1.02	9.82	1.12	1.07
di-14:0	r_o	0.353 (0.008, 0.009)	0.308 (0.004, 0.004)	0.347 (0.008, 0.009)	0.342 (0.006, 0.006)
	χ^2	1.03	4.23	1.06	1.28
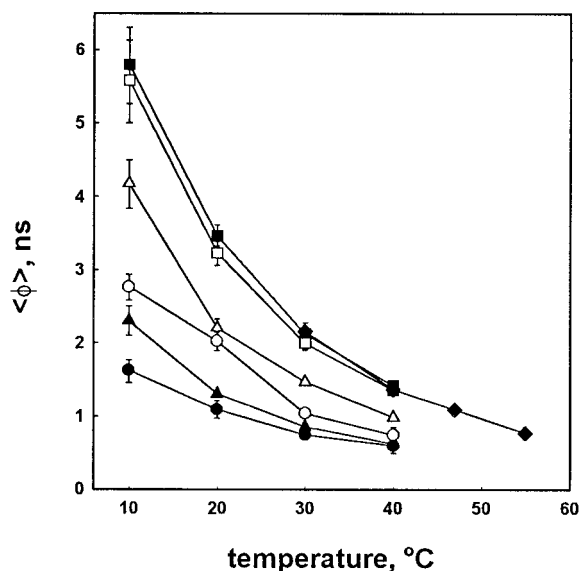
FIGURE 2   Average rotational correlation times, $\langle\phi\rangle$, from analysis of differential polarization data in terms of the sum of two exponential decays plus r_∞; see Eq. 1. ●, di-22:6 PC; ▲, di-20:4 PC; ■, di-18:1 PC; ○, 16:0, 22:6 PC; △, 16:0, 20:4 PC; □, 16:0, 18:1 PC; ◆, di-14:0 PC.

fore all differential polarization data were analyzed in terms of the wobbling-in-cone model and the BRD model. The wobbling-in-cone model has been used by a number of investigators to describe the decay of DPH fluorescence anisotropy in phospholipid bilayers (Lentz, 1993). All anisotropy data were fit with this model via global analysis of data at all four temperatures with r_o globally linked. This analysis produced values of χ^2 ranging from 2.1 to over 10, as shown in Table 2. Values of χ^2 were not improved by using the sum of two exponentials to characterize the decay of total fluorescence intensity, rather than one exponential decay plus a Lorentzian distribution. These values of χ^2 were 2–8 times higher than those of both the sum of exponentials model and the BRD model; therefore the wobbling-in-cone model was not considered an adequate description of the experimental data.

The BRD model was fit to all differential polarization data, utilizing three different analytical procedures: 1) data for a single temperature analyzed with all four fitting parameters ($\langle P_2\rangle$, $\langle P_4\rangle$, $D_\perp$, and r_o) unlinked; 2) data at all four temperatures for each phospholipid composition analyzed simultaneously with r_o globally linked; 3) r_o fixed at 0.38. The effects on $\langle P_2\rangle$, $\langle P_4\rangle$, and $D_\perp$ of these three different treatments of r_o were essentially the same as those reported by Wang et al. (1991), who made a similar comparison in a study involving a smaller number of phospholipid species across a larger range of temperatures. Global analysis significantly reduced the error estimates for all parameters, relative to the results of the single temperature analysis. Fixing the value of r_o at 0.38 in the global analysis resulted in values of χ^2 that were substantially higher than those obtained when r_o was a free, globally linked parameter (results not shown). Values of r_o greater than 0.38 that have

been used by previous investigators (Straume and Litman, 1987a,b) were also examined, but higher fixed values of r_o resulted in even higher values of χ^2. It was not possible to accurately model the anisotropy decay of DPH in these phospholipid bilayers using a single, fixed value of r_o.

A number of studies have presented strong evidence that the value of r_o for DPH depends upon its environment (Lentz, 1993). This environmental dependence is not strictly a function of phospholipid bilayer composition, as Best et al. (1987) report $r_o = 0.385$ for DPH in glycerol and $r_o = 0.35$ for DPH in paraffin. The environmental dependence reported for DPH in phospholipid bilayers is even greater. Studies in which more than one bilayer composition was examined have reported values of r_o from 0.28 to 0.30 (van Langen et al., 1987b), from 0.318 to 0.341 (Wang et al., 1991), and from 0.30 to 0.34 (Muller et al., 1996). Thus the range of values of r_o shown in Table 2 is consistent with other reports in the literature. One possible source of the variation in r_o could be very rapid, unresolved, motion(s) of DPH (Chen et al., 1977). However, this mechanism would predict a decrease in r_o with increased temperature, and no correlation between temperature and r_o was observed in the results of the unlinked, single-temperature analyses. The most likely source of the variation in r_o with bilayer composition is a combination of the factors cited by Muller et al. (1996), which could alter the angle between the absorption and emission dipoles. These include variation in lipid hydration (van Langen et al., 1987a) and alteration of the energy levels of DPH by its environment (Itoh and Kohler, 1987).

A thorough examination of the error surfaces of each phospholipid composition determined that for all compositions there are two solutions to the BRD model, as shown in Table 2. Some of the resulting values of $\langle P_4\rangle$ are quite small, but positive; thus these two solutions are referred to as the "high $\langle P_4\rangle$" and "low $\langle P_4\rangle$" solutions. F tests of the significance of the differences in χ^2 for the two solutions showed that the high $\langle P_4\rangle$ solution was statistically more accurate ($p < 0.04$) for di-14:0 PC and 16:0, 22:6n3 PC, but for all other phospholipid compositions the two solutions are statistically equivalent ($p > 0.3$). Two statistically equivalent solutions to the BRD model for DPH in phospholipid bilayers have been reported by several other investigators (van Langen et al., 1987b, 1989; van Ginkel et al., 1989; Wang et al., 1991).

Although these two solutions are equivalent in terms of their ability to accurately model the anisotropy data, they lead to very different descriptions of the behavior of DPH in these phospholipid bilayers. The low $\langle P_4\rangle$ solution leads to values of r_o and $D_\perp$ that are 5–10% higher than the high $\langle P_4\rangle$ solution. However, the significant difference between the solutions is the resulting orientation distribution function, $f(\theta)$. Examples of these differences are shown in the orientational distribution functions for both solutions for 16:0, 18:1n9 PC at 10°C and 40°C in Fig. 3. The distribution functions, $f(\theta)$, plotted in Fig. 3 are normalized according to $\int f(\theta) \sin\theta \, d\theta = 1$ (Eq. 5b); thus the higher the value
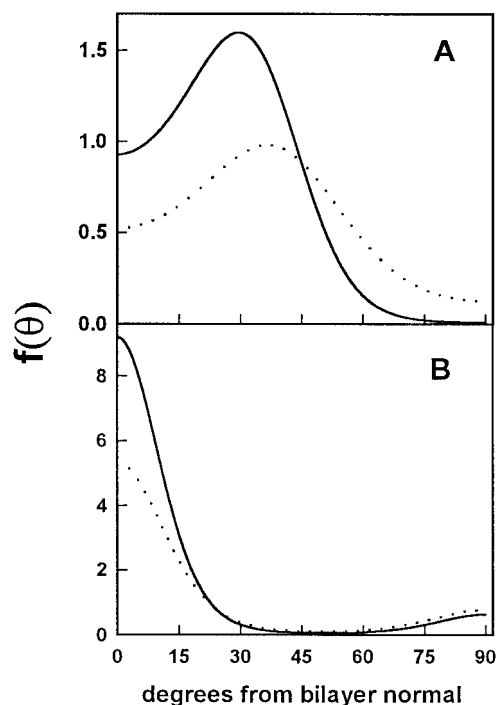
FIGURE 3   Orientational distribution functions for 16:0, 18:1 PC at 10°C (——) and 40°C (·····). (*A*) Low $\langle P_4 \rangle$ solution to BRD model. (*B*) High $\langle P_4 \rangle$ solution to BRD model.

FIGURE 4   Orientational probability functions for 16:0, 18:1 PC at 40°C, corresponding to the low $\langle P_4 \rangle$ solution to the BRD model (——) and the high $\langle P_4 \rangle$ solution to the BRD model (·····). (*A*) $f(\theta) \sin(\theta)$. (*B*) Difference between $f(\theta) \sin(\theta)$ and a random distribution: $f(\theta) \sin(\theta) - f_{random}(\theta) \sin(\theta)$.

of $f(\theta)$ at $\theta = 0$, the greater the area under the curve. The pairs of distribution functions in Fig. 3 show that an increase in temperature from 10°C to 40°C has some similar effects on both types of distributions; the distributions broaden, and the fraction of molecules oriented at large angles from the bilayer normal increases. The net effect of increased temperature for the low $\langle P_4 \rangle$ solutions (Fig. 3 *A*) is a shift of the broad distribution peak away from the bilayer normal, whereas for the high $\langle P_4 \rangle$ solutions (Fig. 3 *B*) it is a redistribution from orientations about the bilayer normal to orientations approximately parallel to the plane of the bilayer. The probability density centered at 90° from the bilayer normal is interpreted as corresponding to the presence of DPH in the bilayer midplane, between the two monolayer leaflets.

A more informative comparison of these two types of distributions is facilitated by comparing the orientational probability distributions, $f(\theta) \sin \theta$. The orientational probability distributions for the high and low $\langle P_4 \rangle$ solutions for DPH in 16:0, 18:1n9 PC at 40°C (Fig. 4 *A*) show the sharp contrast between these two solutions. The high $\langle P_4 \rangle$ solution has two narrow peaks, one near the bilayer normal and the other parallel to the plane of the bilayer. In contrast, the low $\langle P_4 \rangle$ solution has a single broad peak centered at ~45° from the bilayer normal. One of the central questions in this type of investigation has always been, how does the environment of the phospholipid bilayer alter the orientational distribution of the probe molecule from a random distribution? In this context it is instructive to compare the arithmetic dif-
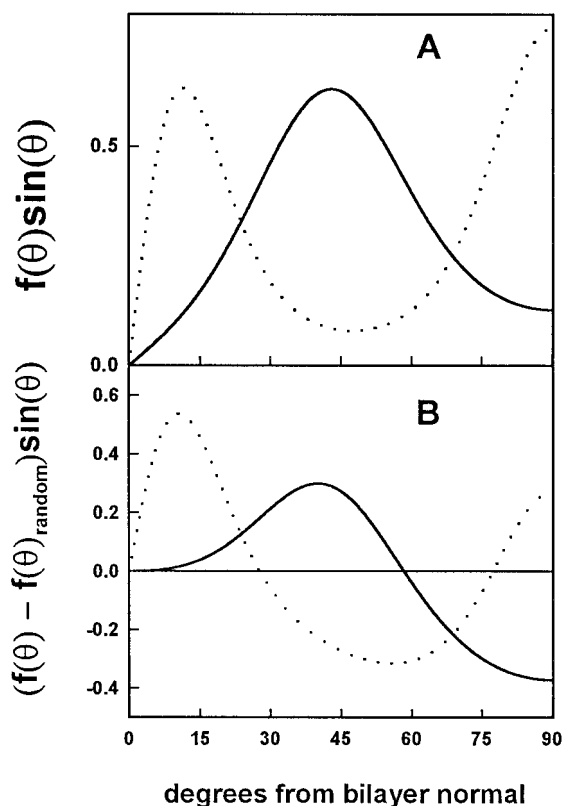
ference between the two distributions in Fig. 4 *A* and a random orientational distribution, as shown in Fig. 4 *B*. Areas below the zero line correspond to angular orientations that DPH is excluded from by the phospholipid acyl chains, whereas areas above the zero line denote angular orientations of DPH that the acyl chains preferentially allow. According to the low $\langle P_4 \rangle$ solution (*solid line*), the net effect of the matrix of acyl chains is to reduce angular orientations between 60° and 90°, relative to a random distribution, and redistribute them into a broad peak between ~10° and 59°. According to the low $\langle P_4 \rangle$ solution, the probability of DPH being aligned near the bilayer normal is approximately equal to that found in a random distribution. In contrast, the high $\langle P_4 \rangle$ solution (*dotted line*) portrays the effect of the acyl chain environment as a reduction in angular orientations between 28° and 78°, with about two-thirds of this probability density transferred to orientations between 0° and 27°, and the balance transferred to orientations between 79° and 90°.

The high and low $\langle P_4 \rangle$ solutions lead to fundamentally different pictures of the phospholipid bilayer. The low $\langle P_4 \rangle$ solution portrays the bilayer as an environment that does not allow a free-tumbling cylinder to be oriented parallel to the bilayer surface or the phospholipid acyl chains, and favors

angular orientations around 45°. The high $\langle P_4 \rangle$ solution depicts the bilayer as an environment that limits orientations around 45° and enhances angular orientations near the bilayer normal and parallel to the bilayer surface. These two very dissimilar orientational distribution functions are both model-dependent in that they result from the particular formulation of the BRD model (Eq. 4) and the choice of $f(\theta)$ (Eq. 6). Best et al. (1987) observed that the type of bimodal distribution corresponding to the high $\langle P_4 \rangle$ solution could result from approximating the full distribution function (Eq. 2) with a function including only $\langle P_2 \rangle$ and $\langle P_4 \rangle$, and inclusion of $\langle P_6 \rangle$ could theoretically produce a minimum in $f(\theta)$ at $\theta = 90°$. However, Pottel et al. (1986) found that a distribution function that included $P_6(\cos \theta)$ was unable to adequately describe DPH anisotropy decays in LC phase bilayers.

Information about the lipid bilayer from other physical techniques suggests that the bimodal orientational distribution corresponding to the high $\langle P_4 \rangle$ solution provides an accurate picture of the hydrophobic core of the bilayer. Numerous deuterium NMR measurements have shown that the terminal six to eight carbon-carbon bonds of a saturated phospholipid acyl chain have the greatest degree of flexibility or conformational freedom (Lefleur et al., 1989). Thus the bilayer midplane may be visualized as a layer 12 to 16 carbon-carbon bonds thick, where the acyl chain conformational degrees of freedom are the greatest, and DPH could orient itself at large angles from the bilayer normal. This picture is difficult to reconcile with the one presented by the low $\langle P_4 \rangle$ solution, where the bilayer reduces the probability of this type of orientation below that encountered in a random distribution. In addition, x-ray diffraction measurements (Grell, 1981) indicate that if DPH interdigitates between the lipid acyl chains, the resulting orientational distribution of DPH must include a large component oriented about the bilayer normal. Finally, the bimodal distribution resulting from the high $\langle P_4 \rangle$ solution is consistent with the orientational distribution obtained from angle-resolved anisotropy measurements on oriented bilayer systems (van Langen et al., 1987b; Deinum et al., 1988; Levine and van Ginkel, 1994). For these reasons we conclude that the high $\langle P_4 \rangle$ solution is the more physically reasonable solution, and it will be used as the basis for analyzing the effects of temperature and acyl chain unsaturation on the equilibrium orientational distribution of DPH in the bilayer.

Effect of unsaturation on the equilibrium orientational distribution of DPH

The results of global analysis of all phospholipid bilayer compositions in terms of the high $\langle P_4 \rangle$ solution to the BRD model are presented in Table 3. The values of $D_\perp$ in Table 3 summarize the effects of temperature and acyl chain unsaturation on DPH motional properties within the context of the BRD model. The temperature-induced changes in $D_\perp$ are very similar to those observed for $\langle \phi \rangle$ in Fig. 2, with $D_\perp$ altered by a factor of at least 2.5 as the temperature rises

TABLE 3 Results of global analysis using the high $\langle P_4 \rangle$ solution to the BRD model

Lipid	°C	$\langle P_2 \rangle$	$\langle P_4 \rangle$	$D_\perp$ (ns^{-1})
di-22:6 PC	10	0.247 (0.016, 0.015)	0.345 (0.024, 0.027)	0.222 (0.025, 0.031)
	20	0.234 (0.012, 0.012)	0.303 (0.023, 0.026)	0.305 (0.029, 0.036)
	30	0.209 (0.013, 0.013)	0.288 (0.021, 0.023)	0.397 (0.034, 0.043)
	40	0.204 (0.012, 0.012)	0.258 (0.025, 0.024)	0.568 (0.045, 0.057)
di-20:4 PC	10	0.206 (0.026, 0.031)	0.237 (0.024, 0.023)	0.105 (0.004, 0.004)
	20	0.162 (0.021, 0.024)	0.211 (0.023, 0.022)	0.173 (0.006, 0.006)
	30	0.124 (0.029, 0.025)	0.206 (0.019, 0.019)	0.263 (0.009, 0.010)
	40	0.151 (0.023, 0.020)	0.173 (0.038, 0.032)	0.357 (0.011, 0.012)
di-18:1 PC	10	0.269 (0.039, 0.042)	0.417 (0.006, 0.008)	0.054 (0.003, 0.003)
	20	0.183 (0.035, 0.020)	0.389 (0.005, 0.008)	0.096 (0.005, 0.005)
	30	0.209 (0.023, 0.013)	0.365 (.0004, 0.008)	0.151 (0.006, 0.006)
	40	0.222 (0.019, 0.017)	0.339 (0.013, 0.012)	0.226 (0.008, 0.009)
16:0, 22:6 PC	10	0.368 (0.011, 0.010)	0.418 (0.015, 0.016)	0.129 (0.010, 0.012)
	20	0.284 (0.014, 0.017)	0.365 (0.015, 0.017)	0.165 (0.011, 0.013)
	30	0.271 (0.010, 0.010)	0.341 (0.012, 0.014)	0.298 (0.017, 0.021)
	40	0.291 (0.006, 0.006)	0.297 (0.011, 0.013)	0.359 (0.016, 0.020)
16:0, 20:4 PC	10	0.199 (0.007, 0.007)	0.407 (0.006, 0.012)	0.082 (0.007, 0.007)
	20	0.188 (0.057, 0.029)	0.356 (0.008, 0.013)	0.135 (0.009, 0.009)
	30	0.190 (0.022, 0.021)	0.342 (0.007, 0.012)	0.201 (0.012, 0.012)
	40	0.179 (0.012, 0.013)	0.309 (0.007, 0.012)	0.290 (0.014, 0.014)
16:0, 18:1 PC	10	0.414 (0.024, 0.022)	0.484 (0.007, 0.014)	0.056 (0.005, 0.005)
	20	0.346 (0.013, 0.013)	0.372 (0.008, 0.011)	0.096 (0.007, 0.007)
	30	0.262 (0.013, 0.012)	0.372 (0.008, 0.011)	0.156 (0.010, 0.010)
	40	0.226 (0.014, 0.010)	0.356 (0.007, 0.012)	0.234 (0.014, 0.014)
di-14:0	30	0.492 (0.010, 0.008)	0.449 (0.021, 0.023)	0.112 (0.015, 0.018)
	40	0.392 (0.007, 0.007)	0.405 (0.018, 0.020)	0.210 (0.023, 0.028)
	47	0.372 (0.007, 0.007)	0.395 (0.018, 0.020)	0.272 (0.029, 0.036)
	55	0.336 (0.035, 0.043)	0.362 (0.018, 0.020)	0.366 (0.036, 0.043)

from 10°C to 40°C. As observed for $\langle\phi\rangle$, $D_\perp$ in 16:0, 18:1 PC and di-18:1 PC has the steepest temperature dependence and reflects the slowest motion of the unsaturated PCs, whereas for di-22:6 PC, $D_\perp$ has the shallowest temperature dependence and reflects the fastest motion. The variation in $D_\perp$ with bilayer composition at 40°C divides DPH motion into four basic groups, with motion increasing in the order di-14:0 PC; 16:0, 18:1 PC; di-18:1 PC < 16:0, 20:4 PC; 16:0, 22:6 PC < di-20:4 PC < di-22:6 PC. This is very similar to the grouping for $\langle\phi\rangle$ observed in Fig. 2.

The significance of the changes in $\langle P_2\rangle$ and $\langle P_4\rangle$ given in Table 3 are most easily understood in the context of the orientational probability distributions, $f(\theta)\sin\theta$. The defining feature of the high $\langle P_4\rangle$ solution of the BRD model is the existence of a bimodal orientational distribution for DPH in a phospholipid bilayer. Changes in the relative width and peak height of these two populations provide a significant basis for comparing the differences in the equilibrium orientation of DPH due to changes in acyl chain composition. The orientational probability distributions for di-14:0 PC and the mixed-chain PCs at 40°C in Fig. 5 A show the range of changes in the two DPH orientational populations induced by progressive unsaturation of the acyl chain at the sn-2 position. The fractional population associated with the bilayer normal decreases in the order di-14:0 PC > 16:0, 18:1 PC > 16:0, 22:6 PC > 16:0, 20:4 PC. In 16:0, 22:6 PC the widths of the distributions are the greatest among the mixed-chain species, as indicated by the significant probability density between 30° and 60° in this phospholipid, and the narrowest distributions are found in 16:0, 18:1 PC.

In general the three mixed-chain PCs in Fig. 5 A resemble each other more than they resemble the distributions for the symmetrically unsaturated PCs shown in Fig. 5 B. Close examination of Fig. 5, A and B, shows that the effect of each unsaturated chain, 18:1n9, 20:4n6, and 22:6n9, is similar in the sn-1 saturated species and diunsaturated species. The 16:0, 18:1 PC and di-18:1 PC (dashed lines) produce the largest population associated with the bilayer normal. At the other extreme, 16:0, 20:4 PC and di-20:4 PC (dotted lines) produce the lowest populations oriented near the bilayer normal, whereas 16:0, 22:6 PC and di-22:6 PC (solid lines) produce intermediate values. The relatively large probabilities for angular orientations between 30° and 60° for di-20:4 PC and di-22:6 PC indicate that in both of these phospholipids, the DPH populations associated with the bilayer normal and the bilayer midplane are both dispersed over a broad angular range. Comparison of Fig. 5 A and Fig. 5 B clearly shows that progressive unsaturation of both acyl chains has a more pronounced effect on the orientational distribution than progressive unsaturation of the sn-2 chain alone.

To assess the extent to which each bilayer restricts the orientational distribution of DPH, the orientational probability distributions for all compositions were compared to a random orientational distribution, as shown in Fig. 5, C and D. The curves in these two panels are the result of subtracting a random probability distribution from the probability
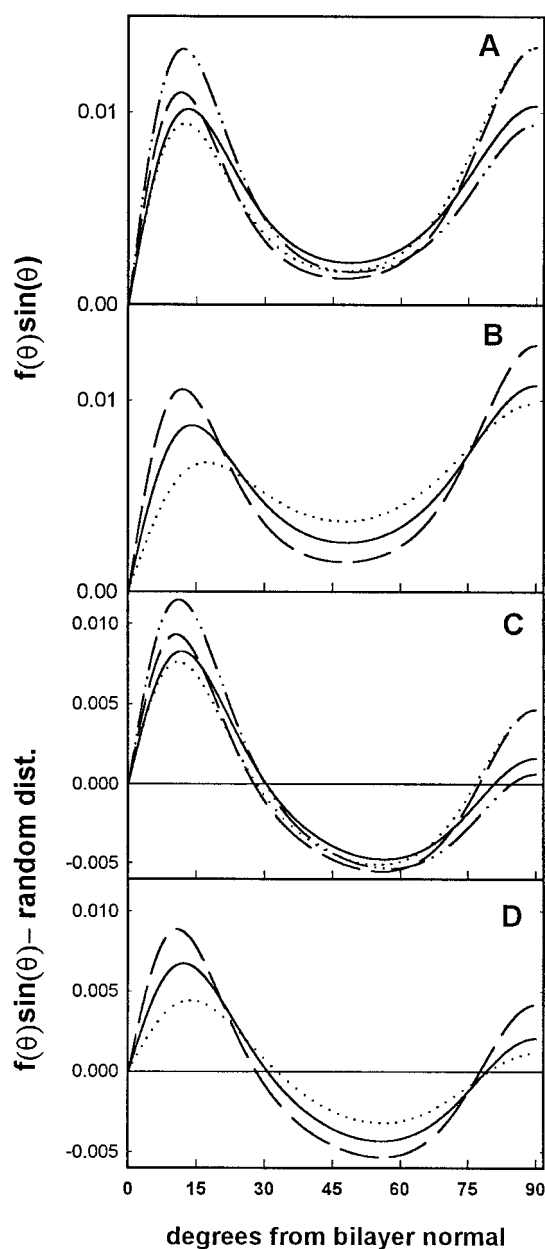

FIGURE 5 Orientational probability distributions for all phospholipid bilayers at 40°C. (A) Probability distributions for di-14:0 PC (– ·· –), 16:0, 18:1 PC (– – –), 16:0, 20:4 PC (·····), and 16:0, 22:6 PC (———). (B) Probability distributions for di-18:1 PC (– – –), di-20:4 PC (·····), di-22:6 PC (———). (C) $f(\theta)\sin(\theta) - f_{\text{random}}(\theta)\sin(\theta)$ for the compositions shown in A. (D) $f(\theta)\sin(\theta) - f_{\text{random}}(\theta)\sin(\theta)$ for the compositions shown in B.

distributions in Fig. 5, A and B. The curves in Fig. 5, C and D, show that bilayers formed from the various phospholipids transfer probability density from angular orientations between ~30° and 75° to orientations less than 30° to varying degrees. In di-14:0 PC, essentially all of the angular orientations greater than 30° are suppressed, whereas in the other phospholipids there is an enhancement above that found in a random distribution at angular orientations near 90°. The curve for di-18:1 PC in Fig. 5 D is very similar to

the curves for the mixed-chain PCs in Fig. 5 *C* in terms of the magnitude of the enhancement of the distribution at 15° and the restriction of the distribution in the intermediate angular range. The three curves in Fig. 5 *D* clearly show that the probability distributions tend toward a random distribution going from di-18:1 PC to di-22:6 PC to di-20:4 PC.

The differences between the various probability distributions in Fig. 5 demonstrate that the phospholipid acyl chains cause the DPH orientational distribution to be nonrandom in a number of different ways. To quantify the degree of orientational restraint imposed by the acyl chains, the parameters f_v and f_{random} were calculated as described in the Experimental Procedures. These parameters facilitate comparison of acyl chain compositions in terms of the extent to which a particular orientational probability distribution is nonrandom, without regard to the particular details that make it nonrandom.

Across the entire temperature range, f_{random} divides the ability of the phospholipids to restrict the equilibrium angular orientation of DPH into several broad groups, as shown in Fig. 6. The low values of f_{random} for di-14:0 PC demonstrate the extent to which orientational distributions in a phospholipid with two saturated acyl chains are restricted relative to unsaturated phospholipids. The next most restrictive group indicated in Fig. 6 consists of the three mixed-chain PCs and di-18:1 PC. The difference between the values of f_{random} for 16:0, 20:4 PC and 16:0, 22:6 PC are only significant at 40°C, but both have significantly higher values of f_{random} than the two 18:1-containing species. It is somewhat surprising that di-18:1 PC is fairly similar to 16:0, 18:1 PC, indicating that the angular orientational freedom of DPH is restricted about equally by a 16:0 chain or a 18:1n9 chain at the *sn*-1 position if the *sn*-2 chain is

18:1n9. At the other extreme, replacement of 16:0 with 20:4n6 in 16:0, 20:4 PC causes an ~50% increase in f_{random}. The very high values of f_{random} for DPH in di-20:4 PC indicate that bilayers formed from this phospholipid are minimally restrictive with respect to the equilibrium angular orientation of DPH. Bilayers formed from di-22:6 PC also provide a much lower level of orientational restraint than the polyunsaturated mixed-chain species. However, the increase in f_{random} upon going from 16:0, 22:6 PC to di-22:6 PC is much less than the increase observed upon going from 16:0, 20:4 PC to di-20:4 PC. The large difference in f_{random} between the two dipolyunsaturated species suggests that there are significant differences in chain-chain interactions between n6 and n3 polyunsaturates.

Previous studies in this laboratory have used the parameter f_v to characterize overall equilibrium ordering experienced by DPH in a phospholipid bilayer (Straume and Litman, 1987a,b, 1988). Further studies have demonstrated that f_v reflects important bilayer properties that depend upon bilayer composition and alter the functional efficacy of the G protein-coupled receptor rhodopsin (Mitchell et al., 1990, 1992; Litman and Mitchell, 1996). Therefore, it is of interest to compare f_v with the overlap between $f(\theta) \sin \theta$ and a random distribution for the large number of acyl compositions and temperatures considered in this study. Fig. 7 shows that for each acyl chain composition, variation in temperature produces a nearly linear relationship between f_v and f_{random}. The clear correlation between these two parameters over the range shown in Fig. 7 demonstrates that the maximum value of $f(\theta)$ is an accurate measure of the overlap of $f(\theta) \sin \theta$ and a random orientational distribution. For bimodal distribution functions of the type resulting from the high $\langle P_4 \rangle$ solution to the BRD model, the maximum
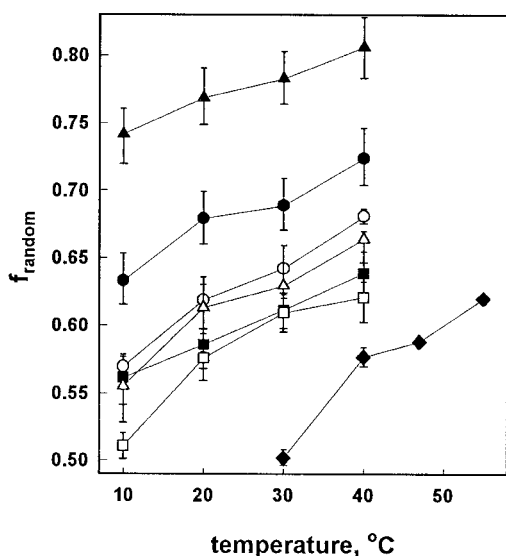

FIGURE 6   Values of the parameter f_{random} as a function of temperature for all phospholipid bilayers. f_{random} was calculated according to Eq. 8. ●, di-22:6 PC; ▲, di-20:4 PC; ■, di-18:1 PC; ○, 16:0, 22:6 PC; △, 16:0, 20:4 PC; □, 16:0, 18:1 PC; ◆, di-14:0 PC.
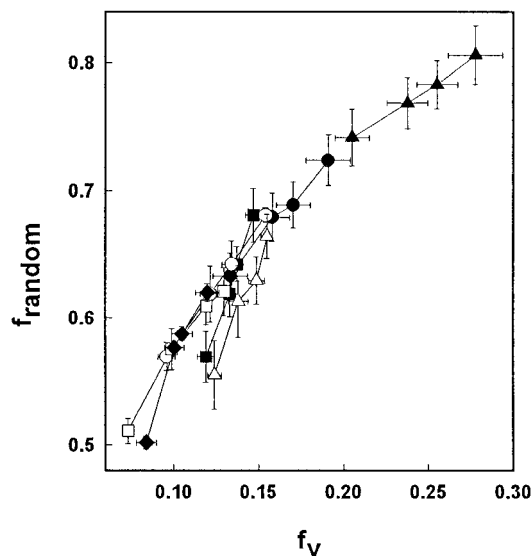
FIGURE 7   Comparison of f_{random} and f_v for all phospholipid species. f_v was calculated according to Eq. 7, and f_{random} was calculated according to Eq. 8. ●, di-22:6 PC; ▲, di-20:4 PC; ■, di-18:1 PC; ○, 16:0, 22:6 PC; △, 16:0, 20:4 PC; □, 16:0, 18:1 PC; ◆, di-14:0 PC.

value of $f(\theta)$ will be at $\theta = 0$; thus calculation of f_v is simple and straightforward once the normalized distribution function is obtained.

Many previous studies that have analyzed DPH dynamic anisotropy in terms of either a simple exponential decay or the wobble-in-cone model have interpreted the residual anisotropy, r_∞, as indicating the extent to which the orientation of DPH is restricted in the bilayer. In this context it is of interest to compare r_∞ and f_v. A plot of r_∞, determined by a fit of a double-exponential function (Eq. 1) to the data, as a function of temperature for all compositions (Fig. 8), suggests a much different grouping of the acyl chain compositions in terms of orientational constraint than was indicated by the analysis of the orientational distribution functions. As in the previous analysis, di-20:4 PC provides the least orientational constraint on DPH, and di-14:0 PC provides the greatest orientational constraint. However, the ordering of the other phospholipids is much different, with 16:0, 20:4 PC, di-18:1 PC, and di-22:6 PC having about the same values of r_∞ at 30°C and 40°C, whereas 16:0, 22:6 PC has about the same value as 16:0, 18:1 PC.

A direct comparison of f_v and r_∞ (Fig. 9) demonstrates the similarities and differences between these two parameters. Both parameters are sensitive to changes in temperature for DPH in the more orientationally restrictive phospholipids, di-14:0 PC and 16:0, 18:1 PC. However, in the least restrictive phospholipids, di-22:6 PC and di-20:4 PC, r_∞ is only minimally different between 10°C and 40°C, whereas f_v changes by almost 50%. These two parameters also report very different effects of acyl chain composition on orientational constraint. Nearly identical values of r_∞ are observed for di-20:4 PC at 10°C, and di-22:6 PC and di-18:1 PC at 40°C. However, the values of f_v under these three different
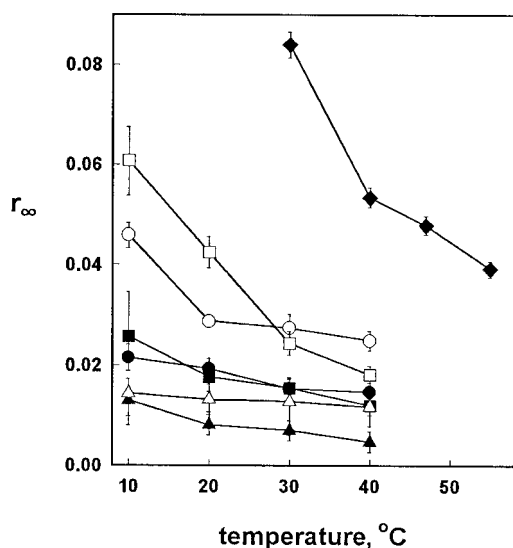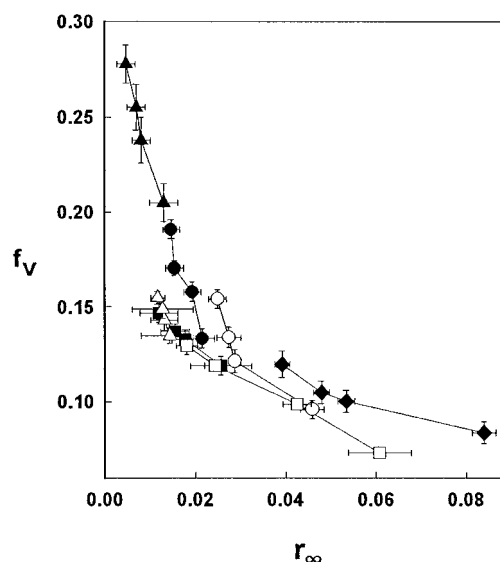

FIGURE 9 The relationship between f_v and r_∞ for all phospholipid bilayers at all temperatures. ●, di-22:6 PC; ▲, di-20:4 PC; ■, di-18:1 PC; ○, 16:0, 22:6 PC; △, 16:0, 20:4 PC; □, 16:0, 18:1 PC; ◆, di-14:0 PC.

conditions varied widely. These differences are most likely due to the fact that r_∞ is related only to $\langle P_2 \rangle$ (van der Meer et al., 1984; Szabo, 1984), whereas f_v depends upon both $\langle P_2 \rangle$ and $\langle P_4 \rangle$. Inspection of Table 3 shows that for the phospholipids where f_v has a greater sensitivity to temperature than r_∞, di-22:6 PC and di-20:4 PC, temperature causes a bigger change in $\langle P_4 \rangle$ than in $\langle P_2 \rangle$, whereas the opposite is true for di-14:0 PC and 16:0, 18:1 PC. The varying relationships between r_∞ and f_v in Fig. 9 may reflect the differential effects of temperature on $\langle P_2 \rangle$ and $\langle P_4 \rangle$ in these phospholipids. Using r_∞ as a single parameter to assess relative orientational order may be equivalent to truncating the series in Eq. 2 after only two terms, whereas f_v includes the information about the orientational distribution contained in the first three terms of the series of Legendre polynomials.

CONCLUSIONS

It is well established that the composition of phospholipid bilayers can greatly alter their functional efficacy. In addition, the phospholipid component of most biological membranes consists of a complicated mixture of different phospholipid headgroups and acyl chain composition. In many biological membranes an appreciable fraction of this mixture consists of phospholipids with highly polyunsaturated acyl chains. It has been proposed that one function of these highly unsaturated species may be to facilitate the formation of lateral domains (Litman et al., 1991; Kariel et al., 1991; Zerouga et al., 1995). If such a mechanism does operate in biological membranes, it will be important to understand the physical properties of the resulting domains, which are rich in highly polyunsaturated acyl chains.

FIGURE 8 Values of the residual anisotropy, r_∞, as a function of temperature. Values of r_∞ were determined via analysis of the differential polarization data with the sum of two exponential decays (Eq. 1). ●, di-22:6 PC; ▲, di-20:4 PC; ■, di-18:1 PC; ○, 16:0, 22:6 PC; △, 16:0, 20:4 PC; □, 16:0, 18:1 PC; ◆, di-14:0 PC.

The present work shows that at the levels of unsaturation considered to be necessary for lateral domain formation, four or more double bonds, all of the bilayer properties that affect DPH lifetime, dynamics, and equilibrium orientational distribution have undergone enormous changes relative to such properties observed in saturated or monounsaturated phospholipids. In addition, these results show that the effect of acyl chain unsaturation is magnified when both acyl chains are highly polyunsaturated. A variety of measurements have shown that the acyl chains of highly dipolyunsaturated phospholipids interact only weakly. Their melting temperatures are quite low (Kariel et al., 1991), very little energy is required to deform bilayers composed of di-20:4 PC, and they have very low interchain van der Waals interactions relative to those of 18:0, 18:1 PC (Needham and Nunn, 1990). The present results support the idea that acyl chains derived from polyunsaturated fatty acids are the most loosely packed phospholipid acyl chains.

The results for di-18:1 PC indicate that the unique properties of the other diunsaturated phospholipids result from their high levels of polyunsaturation rather than from their lack of a saturated acyl chain. Both DPH dynamics and orientational order in di-18:1 PC are more similar to what is observed in the *sn*-1 saturated, *sn*-2 polyunsaturated species than to what is observed in the two dipolyunsaturated species. This implies that the unique chain-chain interactions of polyunsaturated acyl chains are as important to the physical properties of bilayers composed of dipolyunsaturated phospholipids as the absence of strong saturated chain–saturated chain interactions.

In this study DPH anisotropy decays were analyzed in bilayers composed of phosphatidylcholines with acyl chain compositions that spanned the full range of unsaturation found in biological membranes. Analysis in terms of the BRD model provided a description of the anisotropy decay data acquired in all bilayer compositions that was statistically superior to that produced by the wobble-in-cone model. The fact that the BRD model has two distinct solutions that are statistically indistinguishable in no way detracts from its capacity to yield information regarding the detailed angular distribution of a free tumbling bilayer probe. Comparison of these two solutions with a random orientational distribution underlines the dramatically different descriptions of acyl chain packing each solution provides. The high $\langle P_4 \rangle$ solution, which corresponds to a bimodal angular distribution of probe molecules, is consistent with the direct information of acyl chain packing from x-ray diffraction measurements (Grell, 1981) and angle-resolved measurements of DPH fluorescence in oriented planar bilayers (Levine and van Ginkel, 1994). The bimodal orientational distribution, which results from the analytical method we have employed in this study, yields information about acyl chain packing throughout the cross section of the bilayer. Changes in the fractional size and width of the probe population in the bilayer midplane provide information about acyl chain ensemble order in the center of the bilayer, whereas changes in the population oriented about the bilayer normal provide information about ensemble acyl chain packing in the region adjacent to the interfacial region. The result is an analysis of acyl chain packing throughout the depth of the bilayer that complements the information regarding intrachain order from deuterium NMR.

REFERENCES

Alcala, J. R., E. Gratton, and F. G. Prendergast. 1987. Resolvability of lifetime distributions using phase fluorometry. *Biophys. J.* 51:587–596.

Ameloot, M., H. Hendrickx, W. Herreman, H. Pottel, F. van Cauwelaert, and W. van der Meer. 1984. Effect of orientational order on the decay of the fluorescence anisotropy in membrane suspensions. Experimental verification on unilamellar vesicles, and lipid/alpha-lactalbumin complexes. *Biophys. J.* 46:525–539.

Beechem, J. M., E. Gratton, M. Ameloot, J. R. Knutson, and L. Brand. 1991. The global analysis of fluorescence intensity and anisotropy decay data. *In* Second Generation Theory and Programs. Topics in Fluorescence Spectroscopy, Vol. 2, Principles. J. R. Lakowicz, editor. Plenum Press, New York. 241–305.

Bernsdorff, C., A. Wolf, R. Winter, and E. Gratton. 1997. Effect of hydrostatic pressure on water penetration and rotational dynamics in phospholipid-cholesterol bilayers. *Biophys. J.* 72:1264–1277.

Best, L., E. John, and F. Jahnig. 1987. Order and fluidity of lipid membranes as determined by fluorescence anisotropy decay. *Eur. Biophys. J.* 15:87–102.

Caffrey, M. 1993. LIPIDAT. A Database of Thermodynamic Data and Associated Information on Lipid Mesomorphic and Polymorphic Transitions. CRC Press, Boca Raton, FL.

Chen, L. A., R. E. Dale, S. Roth, and L. Brand. 1977. Nanosecond time-dependent fluorescence depolarization of diphenylhexatriene in dimyristoyl-lecithin vesicles and the determination of "microviscosity." *J. Biol. Chem.* 252:2163–2169.

Deinum, G., H. van Langen, G. van Ginkel, and Y. K. Levine. 1988. Molecular order and dynamics in planar lipid bilayers: effects of unsaturation and sterols. *Biochemistry.* 27:852–860.

Grell, E. 1981. Membrane Spectroscopy. Springer-Verlag, Berlin.

Hernandez-Borrell, J., and K. M. W. Keough. 1993. Heteroacid phosphatidylcholines with different amounts of unsaturation respond differently to cholesterol. *Biochim. Biophys. Acta.* 1153:277–282.

Holte, L. L., S. A. Peter, T. M. Sinnwell, and K. Gawrisch. 1995. ^{2}H nuclear magnetic resonance order profiles suggest a change of molecular shape for phosphatidylcholines containing a polyunsaturated acyl chain. *Biophys. J.* 68:2396–2403.

Huster, D., A. J. Jin, K. Arnold, and K. Gawrisch. 1997. Water permeability of polyunsaturated lipid membranes measured by ^{17}O NMR. *Biophys. J.* 73:855–864.

Itoh, T., and B. E. Kohler. 1987. Dual fluorescence of diphenylpolyenes. *J. Phys. Chem.* 91:1760–1764.

Johnson, M. L., and L. M. Faunt. 1992. Parameter estimation by least squares methods. *Methods Enzymol.* 210:1–37.

Kariel, N., E. Davidson, and K. Keough. 1991. Cholesterol does not remove the gel liquid crystalline phase transition of phosphatidylcholines containing two polyenoic acyl chains. *Biochim. Biophys. Acta.* 1062:70–76.

Kinosita, K., Jr., S. Kawato, and A. Ikegami. 1977. A theory of fluorescence depolarization decay in membranes. *Biophys. J.* 20:289–305.

Lakowicz, J. R., H. Cherek, and A. Balter. 1981. Correction of timing errors in photomultiplier tubes used n phase modulation fluorometry. *J. Biochem. Biophys. Methods.* 5:131–146.

Lefleur, M., B. Fine, E. Sternin, P. R. Cullis, and M. Bloom. 1989. Smoothed orientational order profiles of lipid bilayers by ^{2}H nuclear magnetic resonance. *Biophys. J.* 56:1037–1041.

Lentz, B. R. 1993. Use of fluorescence probes to monitor molecular order and motions within liposome bilayers. *Chem. Phys. Lipids.* 64:99–116.

Levine, Y. K., and G. van Ginkel. 1994. Molecular dynamics in liquid-crystalline systems studied by fluorescence depolarization techniques. *In*

The Molecular Dynamics of Liquid Crystals. G. R. Luckhurst and C. A. Veracini, editors. Kluwer Academic, Amsterdam. 537–571.

Lipari, G., and A. Szabo. 1981. Pade approximants to correlation functions for restricted rotational diffusion. *J. Chem. Phys.* 75:2971–2976.

Litman, B. J., E. N. Lewis, and I. W. Levine. 1991. Packing characteristics of highly unsaturated bilayer lipids: Raman spectroscopic studies of multilamellar phosphatidylcholine dispersions. *Biochemistry.* 30:313–319.

Litman, B. J., and D. C. Mitchell. 1996. A role for phospholipid polyunsaturation in modulating membrane protein function. *Lipids.* 31:s193–s197.

Miljanich, G. P., L. A. Sklar, D. L. White, and E. A. Dratz. 1979. Disaturated and dipolyunsaturated phospholipids in the bovine retinal rod outer segment disk membrane. *Biochim. Biophys. Acta.* 552:294–306.

Mitchell, D. C., M. Straume, and B. J. Litman. 1992. Role of *sn-1* saturated, *sn-2* polyunsaturated phospholipids in control of membrane receptor conformational equilibrium: effects of cholesterol and acyl chain unsaturation on the metarhodopsin I:metarhodopsin II equilibrium. *Biochemistry.* 31:662–670.

Mitchell, D. C., M. Straume, J. L. Miller, and B. J. Litman. 1990. Modulation of metarhodopsin formation by cholesterol-induced ordering of bilayer lipids. *Biochemistry.* 29:9143–9149.

Muller, J. M., G. van Ginkel, and E. E. van Faassen. 1996. Effect of lipid molecular structure and gramacidin A on the core of lipid vesicle bilayers. A time-resolved fluorescence study. *Biochemistry.* 35:488–497.

Needham, D., and R. S. Nunn. 1990. Elastic deformation and failure of lipid membranes containing cholesterol. *Biophys. J.* 58:997–1009.

Niebylski, C., and N. J. Salem. 1994. A calorimetric investigation of a series of mixed-chain polyunsaturated phosphatidylcholines: effect of sn-2 chain length and degree of unsaturation. *Biophys. J.* 67:2387–2393.

Pottel, H., W. Herreman, B. W. Van Der Meer, and M. Ameloot. 1986. On the significance of the fourth-rank orientational order parameter of fluorophores in membranes. *Chem. Phys.* 102:37–44.

Salem, N. Jr. 1986. Fatty acids: molecular and biochemical aspects. *In* New Protective Roles For Selected Nutrients, G. A. Spiller and J. Scala, editors. Alan R. Liss Inc., New York. 109–228.

Stinson, A. M., R. D. Wiegand, and R. E. Anderson. 1991. Fatty acid and molecular species compositions of phospholipids and diacylglycerols from art retina membranes. *Exp. Eye Res.* 52:213–218.

Straume, M., S. G. Frasier-Cadoret, and M. L. Johnson. 1991. Least-squares analysis of fluorescence data. *In* Topics in Fluorescence Spectroscopy, Vol. 2. J. Lakowicz, editor. Plenum Press, New York. 177–240.

Straume, M., and B. J. Litman. 1987a. Equilibrium and dynamic structure of large, unilamellar, unsaturated acyl chain phosphatidylcholine vesicles. Higher order analysis of 1,6-diphenyl-1,3,5-hexatriene and 1-[4-(trimethylammonio)phenyl]-6-phenyl-1,3,5-hexatriene anisotropy decay. *Biochemistry.* 26:5113–5120.

Straume, M., and B. J. Litman. 1987b. Influence of cholesterol on equilibrium and dynamic bilayer structure of unsaturated acyl chain phos-

phatidylcholine vesicles as determined from higher order analysis of fluorescence anisotropy decay. *Biochemistry.* 26:5121–5126.

Straume, M., and B. J. Litman. 1988. Equilibrium and dynamic bilayer structural properties of unsaturated acyl chain phosphatidylcholine-cholesterol-rhodopsin recombinant vesicles and rod outer segment disk membranes as determined from higher order analysis of fluorescence anisotropy decay. *Biochemistry.* 27:7723–7733.

Szabo, A. 1984. Theory of fluorescence depolarization in macromolecules and membranes. *J. Chem. Phys.* 81:150–167.

Thurmond, R. L., A. R. Niemi, G. Lindbloom, A. Wieslander, and L. Rilfors. 1994. Membrane thickness and molecular ordering in *Acholeplasma laidlawii* strain A studied by ^{2}H NMR spectroscopy. *Biochemistry.* 33:13178–13188.

Toptygin, D., J. Svobodova, I. Konopasek, and L. Brand. 1992. Fluorescence decay and depolarization in membranes. *J. Chem. Phys.* 96:7919–7930.

Toptygin, D., and L. Brand. 1993. Fluorescence decay of DPH in lipid membranes: influence of the external refractive index. *Biophys. Chem.* 48:205–220.

van der Meer, B. W., R. P. H. Kooyman, and Y. K. Levine. 1982. A theory of fluorescence depolarization in macroscopically ordered membrane systems. *Chem. Phys.* 66:39–46.

van der Meer, B. W., H. Pottel, W. Herreman, M. Ameloot, H. Hendrickx, and H. Schroder. 1984. Effect of orientational order on the decay of the fluorescence anisotropy in membrane suspensions. *Biophys J.* 46:515–523.

van Ginkel, G., H. Van Langen, and Y. K. Levine. 1989. The membrane fluidity concept revisited by polarized fluorescence spectroscopy on different model membranes containing unsaturated lipids and sterols. *Biochimie.* 71:23–32.

van Gurp, M., T. van Heijnsbergen, G. van Ginkel, and Y. K. Levine. 1989. Determination of transition moment directions in molecules of symmetry using polarized fluorescence. II. Applications to pyranine, perylene, and DPH. *J. Chem. Phys.* 90:4103–4111.

van Langen, H., D. Engelen, G. van Ginkel, and Y. K. Levine. 1987a. Headgroup hydration in egg-lecithin multibilayers affects the behavior of DPH probes. *Chem. Phys. Lett.* 138:99–104.

van Langen, H., Y. K. Levine, M. Ameloot, and H. Pottel. 1987b. Ambiguities in the interpretation of time-resolved fluorescence anisotropy measurements on lipid vesicle systems. *Chem. Phys. Lett.* 140:394–400.

van Langen, H., G. van Ginkel, D. Shaw, and Y. K. Levine. 1989. The fidelity of response of 1-[4-(trimethylammonio)phenyl]-6-phenyl-1,3,5-hexatriene in time-resolved fluorescence anisotropy measurements on lipid vesicles. *Eur. Biophys. J.* 17:37–44.

Wang, S., J. M. Beechem, E. Gratton, and M. Glaser. 1991. Orientational distribution of 1,6-diphenyl-1,3,5-hexatriene in phospholipid vesicles as determined by global analysis of frequency domain fluorimetry data. *Biochemistry.* 30:5565–72.

Zerouga, M., L. J. Jenski, and W. Stillwell. 1995. Comparison of phosphatidylcholines containing one or two docosahexaenoic acyl chains on properties of phospholipid monolayers and bilayers. *Biochim. Biophys. Acta.* 1236:266–272.